so that the domain walls traversing there always proceeded in the same direction.

It is very likely that the structural change that we have found would give important effects on every process of polarization reversal in $BaTiO_3$. Here we present a bold view for the mechanism of bringing about the anomalous structure change. Generally the directions of spontaneous polarization before and after its reversal are related to each other by a symmetrical operation of rotation. However, it is agreed that the anisotropy of most ferroelectrics is so high that the rotation of the polarization vector within the wall will not occur. In the case of room-temperature structure of $BaTiO_3$, e.g., $c/a = 1.01$, the anisotropy does not seem so high that the possibility of rotation of dipoles in a crystalline medium should be absolutely excluded, but it is rather realistic to assume that the rotation mechanism contributes in part to the polarization reversal. If any, the crystalline portions relevant to polarization reversal would be subjected to pure shear stress X_5 or its equivalents, because rotation of polarization takes place in an anisotropic medium. Then the polarization P_1 directed normal to the existing polarization P_3 will be developed as a result of piezoelectric coupling through a torsion modulus d_{15} or d_{24}, e.g.,[3]

$$P_1 = d_{15}X_5.$$

This will be naturally accompanied by the pseudo-monoclinic deformation of the crystalline portions. It is noted that the proposed mechanism is concerned with dynamical process of domain switching. It seems to explain qualitatively all optical characters mentioned before. Especially it is of particular interest that the origin of the character (4) is understandable if we relate one direction of domain movement with right-handed rotation and necessarily the reversed direction with left-handed one.

[1]R. C. Miller and A. Savage, Phys. Rev. Letters 2, 294 (1959).

[2]R. C. Miller and A. Savage, J. Appl. Phys. 31, 662 (1960).

[3]It may be noticed that d_{15} is about 11 and five times as large as d_{31} and d_{33}, respectively [D. Berlincourt and H. Jaffe, Phys. Rev. 111, 143 (1958)].

TWO-QUANTUM ABSORPTION SPECTRUM OF KI[†]

J. J. Hopfield,* J. M. Worlock,‡ and Kwangjai Park

Department of Physics, University of California, Berkeley, California

(Received 15 August 1963; revised manuscript received 30 September 1963)

We have measured the two-quantum absorption spectrum of crystalline KI in the vicinity of the fundamental absorption edge. Two-quantum absorption is a nonlinear phenomenon in which two quanta are simultaneously absorbed in an electronic transition, energy being conserved only between the electronic system and the two quanta. The electronic system is transparent to either quantum alone. Such a process has been observed by Kaiser and Garrett[1] and others, and theoretically investigated by Kleinman[2] and Braunstein.[3] In previous experiments, the absorbed quanta have both been obtained from a narrow-band laser source.

In this experiment, a continuous source of ultraviolet light has been used, allowing a broad spectrum to be investigated. To our knowledge, this is the first experimental demonstration of the utility of this technique in the range of optical energies.

The two-quantum absorption spectrum should contain as much information about a system (e.g., a solid) as does the ordinary one-quantum spectrum. Because the selection rules are very different (even-parity transitions for two-photon absorption versus odd-parity transitions for one-photon absorption), the two methods of investigation are complementary rather than identical.

The fundamental absorption edge of crystalline KI has not been well understood. Different theoretical models[4] predict similar one-photon absorption spectrum singularities, but quite different two-quantum spectra. This experiment was designed to provide a basis for choice among the various theories, and to allow the experimental study of the absorption process in bulk
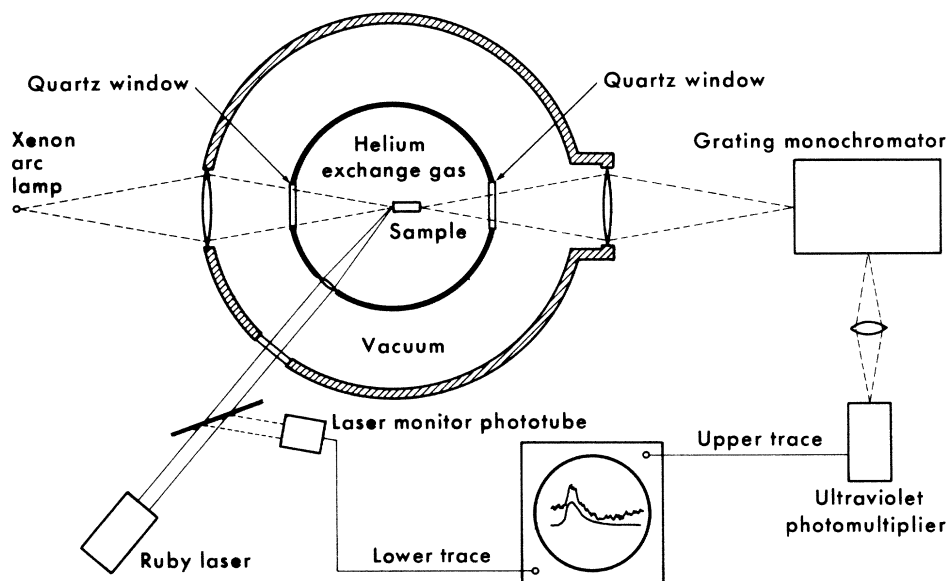
FIG. 1. Schematic diagram of the experiment.

crystalline material rather than in the usual evaporated films.

The basic experimental design is shown in Fig. 1, which is simplified by the omission of several filters designed to reject stray laser light and prevent ultraviolet coloration of the sample. The samples were cleaved from Harshaw KI crystals to a size of approximately 2 ×3×25 millimeters. The laser (Lear Siegler, Inc. LS-4) was operated at an output of about 15 joules per pulse. The ultraviolet and laser beams were kept within the sample by total internal reflection.

Two-quantum absorption, if it occurred at the wavelength being monitored, resulted in a decrease in ultraviolet transmission proportional to the laser intensity. A typical signal (ultraviolet wavelength 2770 Å, sample at liquid nitrogen temperature) is shown in Fig. 2. The lower trace represents the laser intensity. The upper trace shows the simultaneous decrease in ultraviolet intensity; the polarity of this signal was reversed. The peak decrease in intensity was in this case about one part in 500. The similarity of shape of the two signals indicates that the effect is proportional to the laser intensity. The signal has also been shown to have the expected proportionality to ultraviolet intensity.

The experimental results are conveniently represented as an apparent optical density proportional to the laser intensity. The spectra of

this specific induced optical density (optical density/incident laser flux) are shown in Fig. 3 for KI crystals at two temperatures. (Conversion of Optical densities into absorption constants would be appropriate if the laser flux were constant throughout the lengths of the crystals. Since the surfaces are not perfect, there is some leakage, which may be different in the two crystals, and the two curves are not necessarily directly comparable.)

Some characteristic energies of one- and two-photon absorption are expected to be common.
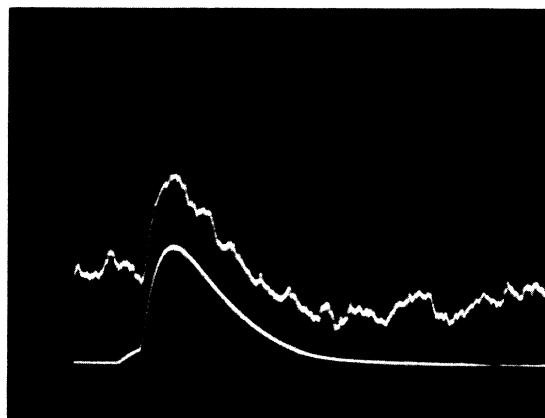

FIG. 2. Typical dual-trace oscillogram showing the ultraviolet (upper trace) and laser (lower trace) intensities. Sweep speed 2 cm/msec. Both signals have passed through 0.2-msec high-cut filters.
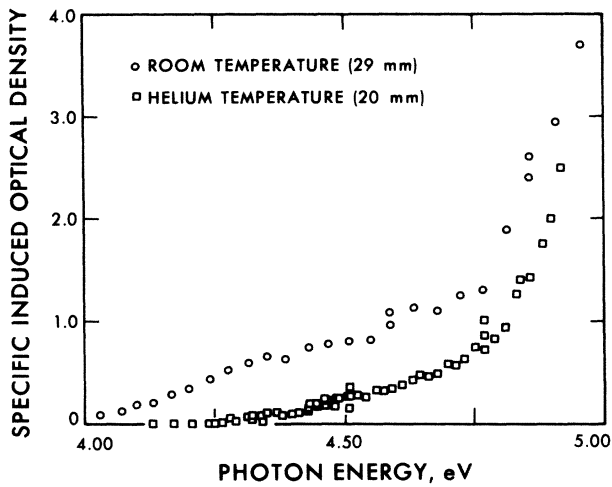
FIG. 3. Two-photon absorption spectra of KI at
room temperature and liquid helium temperature.
The ordinate is approximately the percentage de-
crease in transmission for an incident laser flux of
$1/3$ MW/cm^2. The resolution is 0.03 eV. The lengths
of the two crystals are shown in the figure.

FIG. 4. One- (see reference 5) and two-photon
absorption spectra of KI at low temperature. The
abscissas differ by 1.79 eV, the energy of a ruby-
laser photon.

Figure 4 shows a superposition of a single-photon
absorption spectrum of Teegarden[5] and the pres-
ent two-photon data. The temperature shift be-
tween the two temperatures compared is small,
~0.05 eV.[6]

Several observations ought to be made concern-
ing Figs. 3 and 4. (1) The two-quantum absorp-
tion seems to exhibit two edges having thresholds
near characteristic energies observed in one-
quantum absorption. (2) The low-energy two-
photon edge shifts 0.25 eV toward higher ener-
gies between room temperature and helium tem-
perature. The high-energy two-quantum edge
shifts much less. In comparison, the lowest
energy (one-quantum) exciton band (5.8 eV)
moves about 0.25 eV between room and helium
temperature, while the high-energy peak (6.7
eV) moves only about 0.1 eV.[6] (3) The two-
quantum continuum absorption coefficient for a
two-band allowed transition model is given by

$$\alpha_2(E_{uv}; E_1) = \alpha_1(E_{uv} + E_1)(4\pi e^2\hbar^2/m^*)(E_{uv} + E_1 - E_0)$$

$$\times (1/E_1)^2(1/E_1 + 1/E_{uv})^2 U, \quad \text{for } (E_{uv} + E_1 - E) \geqslant 0,$$

where α_1 and α_2 are the one- and two-quantum
absorption coefficients, E_{uv} and E_1 the ultraviolet
and laser quantum energies, E_0 the band gap, and
U the energy density of the laser beam. This
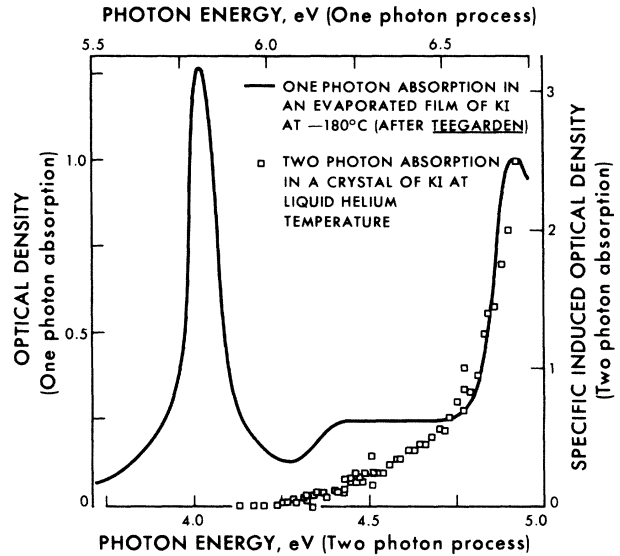crude model predicts, from the one-quantum ab-

sorption, an α_2 of 1×10^{-3} cm^{-1} at helium tem-
perature and 4.70 eV, which compares favorably
to the value of 2.5×10^{-3} cm^{-1} estimated from
the experimental data. (4) There is evidence
for a small (~20% above the continuum absorption)
peak at 6.21 eV which has been interpreted as a
Wannier $2S$ exciton.[6] If such a state exists, the
two-photon curve should exhibit a peak at an
equivalent energy corresponding to the Wannier
$2P$ state. Our data are too noisy to say whether
or not such a peak is present. (5) A striking
feature of the two-photon absorption is the ab-
sence of any absorption corresponding to the ex-
citon peak at 5.8 eV. The data of Fig. 4 have
been extended to 3.9 eV but show no further ab-
sorption. The excitation and Wannier exciton
models are both consistent with this result;
neither requires an even-parity state near the
ground (odd-parity) exciton state. The transfer
model, on the other hand, does require such a
nearby even-parity state and is therefore not
consistent with this result. (6) It was attractive
to associate the rise in two-quantum absorption
above 4.8 eV with the corresponding peak in one-
photon absorption at 6.7 eV. If the one-photon
peak is the spin-orbit split (halogen doublet)
partner of the exciton peak at 5.8 eV, the ab-
sence of two-photon absorption associated with
one peak implies the absence of such absorption
associated with the other.

The signal-to-noise problem, well illustrated in Fig. 2, is currently being studied in an attempt to search for fine structure in the absorption edge.

The authors would like to thank those many persons who have lent us encouragement, advice, and equipment.

*Alfred P. Sloan Foundation Fellow.
‡National Science Foundation Postdoctoral Fellow.
[1]W. Kaiser and C. G. B. Garrett, Phys. Rev. Letters 7, 229 (1961).
[2]D. A. Kleinman, Phys. Rev. 125, 87 (1962).
[3]R. Braunstein, Phys. Rev. 125, 475 (1962).
[4]A. W. Overhauser, Phys. Rev. 101, 1702 (1956); D. L. Dexter, Phys. Rev. 108, 707 (1957); R. S. Knox and N. Inchauspé, Phys. Rev. 116, 1093 (1959); F. Fischer, Z. Physik 160, 194 (1960).
[5]K. Teegarden, Phys. Rev. 108, 660 (1957).
[6]F. Fischer and R. Hilsch, Nachr. Akad. Wiss. Göttingen, IIA. Math. Physik. Kl. No. 8, 241 (1959).

DISTURBANCE OF PHONON DISTRIBUTION IN HIGH ELECTRIC FIELDS

A. Zylbersztejn and E. M. Conwell*
Laboratoire De Physique De L'Ecole Normale Superieure, Paris, France
(Received 8 August 1963)

The rate of phonon generation may be calculated from the well-known expressions for the rates of scattering of electrons with phonon emission and absorption, respectively.[1] For the conditions of interest, electron energy is too low for optical phonon emission, and carrier concentration is fairly high. We may therefore take for the distribution function of the electrons in the ith valley a Maxwell-Boltzmann distribution $f^{(i)} = \{n/N_c(T_e^{(i)})\}\exp[-\epsilon/k_0 T_e^{(i)}]$, where $N_c(T_e^{(i)})$ is the "effective density of states" in the ith valley. We shall neglect the asymmetric part of the electron distribution and of the disturbed phonon distribution since these are expected to be small. When the phonon disturbance is not too large, the phonon lifetime should be given by the boundary scattering value L/u_α, where u_α is the appropriate sound velocity. Taking the steady-state value N_q of phonons with wave vector q as the product of the generation rate and this lifetime, we find for $\hbar u_\alpha q \ll k_0 T_e^{(i)}$

$$N_{q\alpha} = \left[\sum_{i=1}^{g} F_\alpha^{(i)}\right] \Big/ \left[1 + \sum_{i=1}^{g} F_\alpha^{(i)} \hbar u_\alpha q/k_0 T_e^{(i)}\right], \quad (1)$$

where g is the number of valleys, and

$$F_\alpha^{(i)} = \tfrac{1}{2}L \frac{m_t^{3/2} m_l^{1/2}}{\pi \hbar^4 \rho u_\alpha^2} \frac{n^{(i)}}{N_c(T_e^{(i)}) k_0 T_e^{(i)}} \frac{\Xi_\alpha^2}{C^{1/2}(\theta_i)}$$

$$\times \exp\{-[\hbar^2 q^2/8m k_0 T_e^{(i)}]C(\theta_i)\}, \quad (2)$$

$$C(\theta_i) = \sin^2\theta_i + (m_t/m_l)\cos^2\theta_i, \quad (3)$$

θ_i being the angle between $\vec{q}$ and the symmetry axis of the ith valley. For longitudinal waves $\alpha = l$ and and $\Xi_l = \Xi_d + \Xi_u \cos^2\theta_i$; for transverse waves $\alpha = t$ and $\Xi_t = \Xi_u \sin\theta_i \cos\theta_i$, the Ξ's being the deformation potential constants defined by Herring and Vogt.[1] It is seen that, for the $F_\alpha^{(i)}$ not large compared to unity, which we shall assume to be the case throughout this treatment, (1) is not in a form for which we may say the phonon distribution has a new temperature.

N_{ql} and N_{qt} were calculated for n-Ge, for several directions of q, with current assumed in the [100] direction, in which case $T_e^{(i)}$ is the same for all valleys. T_e was taken as $10T_{\text{lat}}$, or $40°$, and $\hbar\omega_q/k_0 T_{\text{lat}}$ was taken as 2. For q in the [100] direction, it was found that $F_t^{(i)} = 3.32nL/5 \times 10^{14}$ for L in cm, n in cm^{-3}. $F_l^{(i)}$ for this direction was quite small. For q in the [111] direction, $F_l^{(111)} = 12.1nL/5 \times 10^{14}$, but it is much smaller for the other three valleys. The corresponding quantity for transverse waves is 0 for the [111] valley, and small for the other three valleys. Despite the large anisotropy of N_{ql} and N_{qt} individually, their sum has small anisotropy. For $L = 1$ cm, $n = 5 \times 10^{14}$/cm³, the sum is $\simeq 4$ for q in the [100] direction, 5.5 for q in the [111] direction.

With N_q given above, one may calculate from the usual formalism[1] the relaxation-time tensor and the mobility, which is a scalar for current in the [$\bar{1}$00] direction, as functions of T_e. In turn, T_e may be determined by the familiar technique
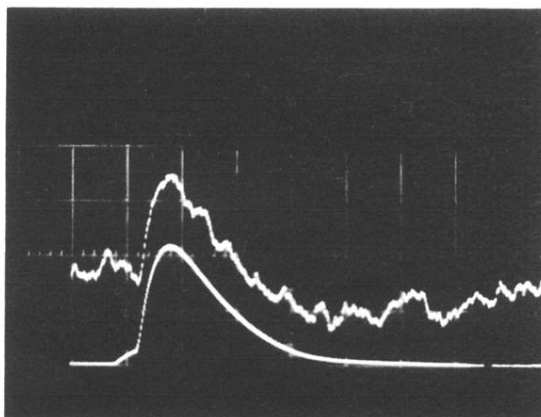
FIG. 2. Typical dual-trace oscillogram showing the ultraviolet (upper trace) and laser (lower trace) intensities. Sweep speed 2 cm/msec. Both signals have passed through 0.2-msec high-cut filters.